

Effects of redox properties and acid–base properties on isosynthesis over ZrO₂-based catalysts

Yingwei Li, Dehua He,* Qiming Zhu, Xin Zhang, and Boqing Xu

Department of Chemistry, Tsinghua University, Beijing 100084, China

Received 11 June 2003; revised 8 September 2003; accepted 24 September 2003

Abstract

ZrO₂-based catalysts doped with CeO₂ or Y₂O₃ were prepared by coprecipitation and the catalytic performance of each was evaluated in the selective synthesis of isobutene and isobutane (i-C₄) from CO hydrogenation at 673 K, 5.0 MPa, and 650 h⁻¹. The physical properties and chemical properties (acid–base and redox) of the catalysts were systematically characterized and related to the catalytic performance. The catalytic activities and selectivities of the ZrO₂-based catalysts varied with the quantity of CeO₂ and Y₂O₃ doped. The physical properties, such as surface areas, cumulative pore volumes, average pore diameters, crystal phases, and crystal sizes had no appreciable effects on the catalytic performance of the catalysts. Temperature-programmed reduction (TPR) of H₂ measurements showed that the addition of CeO₂ or Y₂O₃ into ZrO₂ enhanced the reduction properties of the catalysts. The highest activities and C₄ selectivities in total hydrocarbons were obtained over the catalysts which have a maximum amount of H₂ consumption measured by TPR technology for both CeO₂- and Y₂O₃-doped ZrO₂-based catalysts. The selectivity to i-C₄ in total hydrocarbons also achieved a maximum over the catalyst (50% CeO₂-doped ZrO₂) which has a maximum amount of H₂ consumption in the TPR for the CeO₂-ZrO₂ mixed oxide catalysts. For the Y₂O₃-ZrO₂ mixed oxide catalysts, high selectivities to i-C₄ in total hydrocarbons were obtained over the catalysts with the contents of doped Y₂O₃ ranging from 4.5 to 8.6%; whereas the maximum H₂ consumption was attained at 8.6% Y₂O₃ doped. The acid–base properties also played a significant role in determining the activity and selectivity of the ZrO₂-based catalysts in the CO hydrogenation. A coordination of redox and acid–base properties accounts for the remarkable improvement of reaction activities and selectivities over the CeO₂- or Y₂O₃-doped ZrO₂-based catalysts in this investigation.

© 2003 Elsevier Inc. All rights reserved.

Keywords: CO hydrogenation; Zirconia based; Isobutene; Acid–base; Redox

1. Introduction

Isosynthesis has been referred to as the reaction that selectively converts coal or natural gas-derived syn-gas (CO + H₂) to i-C₄ hydrocarbons (isobutene and isobutane). It has attracted much attention in recent years because of a worldwide shortage of isobutene and isobutane which are extracted from a limited C₄ stream of a petroleum cracking process at the present time [1]. Thorium dioxide (ThO₂) and zirconium dioxide (ZrO₂) have been shown to be the two most active catalysts for this reaction [2,3]. Recent research has mostly focused on zirconia-based catalysts because of their absence of radioactivity and high selectivity to isobutene [4–10].

Zirconia is considered to be a unique metal oxide which explicitly possesses special chemical properties such as acidic and basic properties and redox properties [11]. The effects of acidic and basic properties on the catalytic performance of isosynthesis have been extensively studied over zirconia-based catalysts [5–10]. Maruya and co-workers [5] investigated the effects of various metal promoters. They found that the addition of highly electronegative oxides such as SiO₂ and Nb₂O₅ resulted in a decrease of isobutene with an increase of methane. ZrO₂ modified with NaOH promoted the selective formation of i-C₄ hydrocarbons. They suggested that the strong basicity of the catalysts was significant for the formation of i-C₄ hydrocarbons. The lower selectivity to isobutene over SiO₂ or Nb₂O₅-doped ZrO₂ catalysts was due to the decrease of basicity with the increase in acidity of the mixed oxides because both SiO₂ and Nb₂O₅ have a higher electronegativity than ZrO₂. But that work was performed at very low CO conversions (0–5%) [5].

* Corresponding author.

E-mail address: hedeh@mail.tsinghua.edu.cn (D. He).

Feng and co-workers [6] synthesized zirconia-based catalysts with different acid–base properties and studied the relation between isosynthesis activity and acid–base properties of the catalysts. They found that the product distribution of CO hydrogenation depended on the acid–base properties of the catalysts. It was suggested that a high ratio of basic to acidic sites is a requirement for an active catalyst to produce isobutene and isobutane from CO hydrogenation.

Jackson and Ekerdt [7] investigated the effect of the acidity on the isosynthesis reaction conducted at 698 K and 35 atm. The acid strength of the catalysts was altered by the additives, including H_2SO_4 and Sc_2O_3 . A balance of acidic and basic properties on ZrO_2 was suggested to be necessary for the formation of isobutene and isobutane.

Our previous works [8–10] suggested the importance of the coordination of acid–base active sites in the isosynthesis reaction. The acidic sites were found to be responsible for the activation of CO to start the reaction and the formation of *n*-C₄ hydrocarbons. However, the basic sites are significant for the formation of *i*-C₄ hydrocarbons. An appropriate amount of acidic and basic sites and a ratio of basic to acidic sites on the catalysts are significant for the direct synthesis of *i*-C₄ hydrocarbons from CO hydrogenation.

Although the effects of acid–base properties of zirconia-based catalysts on isosynthesis have been extensively investigated, very little research has been done on redox properties of zirconia-based catalysts for the isosynthesis. Jackson and Ekerdt [7] studied the effect of oxygen vacancies on the isosynthesis reaction. The oxygen vacancy availability was altered by the addition of dopants Y_2O_3 and CaO in varying concentrations. The most active catalysts were those in which ionic conductivity was at a maximum, suggesting that vacancies of the crystal lattice in the catalysts play an important role in the reaction. However, the redox and acid–base properties of these Y_2O_3 - and CaO-promoted zirconia catalysts have not been systematically characterized and studied, making it difficult to understand the true effect of oxygen vacancies on the isosynthesis reaction.

Despite a large number of investigations on the isosynthesis reaction reported in the past, a systematic investigation of the influence of physical and chemical properties (acid–base and redox) of zirconia-based catalysts upon the catalytic performance has not been reported so far. A systematic comprehension of the influence of physical and chemical properties upon the catalytic performance of zirconia-based catalysts is necessary, since it has been reported that both physical and chemical properties of the catalysts affect the activities and selectivities of isosynthesis [9,12]. The primary objective of present work is to identify the function of redox properties on isosynthesis activities and selectivities through a systematic investigation of the effects of physical, acid–base, and redox properties on the catalytic performance of zirconia-based catalysts in the isosynthesis. The redox properties were modified by doped ZrO_2 with various quantities of CeO_2 and Y_2O_3 , since it has been reported that the redox properties of zirconia could be largely improved due to an

increased lattice oxygen mobility [13–16] for a distortion of the oxygen sublattice by the incorporation of Ce^{4+} and Y^{3+} into the crystal lattice of ZrO_2 . The texture, crystal structure, reduction, and acid–base properties were systematically investigated using N_2 physisorption, X-ray diffraction (XRD) and Raman spectra, temperature-programmed reduction (TPR), and desorption (TPD) study. In parallel, steady-state isosynthesis activities and selectivities were measured to relate the observed catalytic performance to the physical and chemical properties characterized on these CeO_2 - and Y_2O_3 -doped ZrO_2 catalysts. The physical and chemical properties required for the isosynthesis reaction were identified and are discussed in this paper.

2. Experimental

2.1. Preparation of catalysts

Hydrous zirconia was prepared by adding dropwise a solution of ZrOCl_2 (0.15 M) into a well-stirred ammonium solution (2.5%) at room temperature. The pH value during precipitation was carefully controlled at 10. The precipitate formed as described above was collected by filtering and washing with deionized water until there was no detectable Cl^- . The gel was dried at 378 K for 24 h and then calcined at 823 K for 3 h in air. CeO_2 - ZrO_2 and Y_2O_3 - ZrO_2 mixed oxides were synthesized by coprecipitation of a mixed solution (0.15 M) of ZrOCl_2 and various additives, cerium or yttrium nitrate salts, with ammonium solution (2.5%), and the above procedure was followed. The concentration of the additives, such as CeO_2 , was changed in a systematic manner by changing the ratio of Zr and Ce in the mixed solution. The prepared catalysts are listed in Table 1.

2.2. Characterization of catalysts

Powder X-ray diffraction patterns were recorded on a Brüker D8 advance powder diffractometer using nickel-filtered Cu-K_α radiation. The crystal size was determined by means of the X-ray line broadening method using the Scherrer equation [17]. Raman spectra were obtained at room temperature with a microscopic confocal Raman spectrometer (Renishaw, RM 2000). The 514-nm line from an argon ion laser was used as the excitation source. Incident powers of about 5 mW on the sample were used.

N_2 adsorption/desorption isotherms at 77 K were obtained on a Micromeritics ASAP 2010C analyzer. Before measurement, the samples were degassed at 473 K for 6 h.

The acid–base properties of the catalysts were measured by temperature-programmed desorption of ammonia and carbon dioxide, respectively. TPD experiments were carried out in a flow-type apparatus at atmospheric pressure. Typically, a 100-mg sample was treated at its calcined temperature (823 K) in a highly pure helium ($\geq 99.995\%$) flow for 0.5 h and then saturated with a 1.0% NH_3/He mixture

Table 1
Physical properties of CeO₂-ZrO₂ and Y₂O₃-ZrO₂ mixed oxide catalysts

Catalyst	Content of CeO ₂ or Y ₂ O ₃ ^a (mol%)	S _{BET} (m ² /g)	Cumulative pore volume ^b (cm ³ /g)	Average pore diameter ^c (nm)	Crystal size (nm)
CeO ₂ -ZrO ₂	0	55	0.212	11.8	15
	12	85	0.12	3.9	8
	50	86	0.086	3.1	5
	88	75	0.065	3.1	7
	100	60	0.053	3.3	13
Y ₂ O ₃ -ZrO ₂	2.5	81	0.148	5.1	11
	4.5	115	0.194	4.6	8
	6.2	119	0.157	3.6	9
	8.6	120	0.157	3.9	8
	12	130	0.162	3.5	5

^a CeO₂/(CeO₂ + ZrO₂) or Y₂O₃/(Y₂O₃ + ZrO₂).

^b BJH desorption cumulative pore volume of pores in the range 1.7–300 nm.

^c BJH desorption average pore diameter.

or highly pure CO₂ (99.99%) flow after cooling to 373 K. After being flushed with He at 373 K for 1 h to remove physisorbed NH₃ or CO₂, the sample was heated to 823 K at a rate of 20 K/min in a helium flow of 60 cm³/min. The desorbed NH₃ or CO₂ was measured by a QMS (MSC 200).

Temperature-programmed reduction studies were carried out in a conventional system equipped with a thermal conductivity detector (TCD). The amount of catalyst used was 100 mg in all cases. The catalyst samples were treated in Ar at 823 K for 0.5 h before TPR was performed. TPR was carried out in a flow of 5% H₂/Ar (20 ml/min) at a heating rate of 10 K/min. A cold trap (203 K) was placed before the TCD to remove water produced during the reaction. The hydrogen consumption was calibrated using TPR of copper oxide (CuO) under the same conditions.

2.3. Reaction procedure

The hydrogenation of CO was carried out in one specially designed high-pressure flow fixed-bed reactor at 5.0 MPa, 673 K, and 650 h⁻¹. It is a quartz-lined stainless-steel tubular reactor in which the quartz line (i.d. = 8 mm) was tightly fixed in a stainless-steel tube. A stainless-steel tubular reactor was normally used in most research on the isosynthesis reaction that was performed at a high pressure [6–9]. Here, the quartz-lined stainless-steel tubular reactor was used because our previous work [18] showed that the stainless-steel materials seriously affected the actual catalytic performance of catalyst. The selectivity to *i*-C₄ hydrocarbons on the stainless-steel tubular reactor was much lower than that on the quartz-lined stainless-steel tubular reactor with an increase of C₁–C₃ hydrocarbon products [18]. The pelletized catalyst (1 g) was crushed and sieved to particles (20–40 mesh) and then packed in the reactor. Before the reaction was conducted, the catalyst was pretreated in a stream of N₂ at 673 K for 3 h. After the temperature was cooled to 623 K in N₂, syn-gas (CO/H₂ = 1) was introduced into the reactor. Synthesis gas (CO/H₂ = 1) was purified by removing metal carbonyls and water with an activated charcoal trap and a molecular sieve trap, respectively. The reactor

effluent was reduced to atmospheric pressure and then injected into two on-line gas chromatographs. One equipped with TCD was used to separate CO, CH₄, CO₂, CH₃OH, and CH₃OCH₃ through a GDX-101 column, and another equipped with FID and a 30 m × 0.53 mm Al₂O₃ capillary column was applied to separate hydrocarbons.

3. Results and discussion

3.1. Physical properties of the mixed oxide catalysts

Several physical properties of the catalysts were measured and the results are summarized in Table 1. Pure ZrO₂ prepared in this study had a moderate specific area ca. 55 m²/g. Incorporation of CeO₂ or Y₂O₃ to ZrO₂ both increased the specific area. The CeO₂-ZrO₂ mixed oxides had similar specific areas at the contents of CeO₂ doped in this investigation. The specific areas of Y₂O₃-ZrO₂ mixed oxides increased with an increase in the content of Y₂O₃. However, the specific areas were almost the same when the content of Y₂O₃ varied from 4.5 to 8.6% in the Y₂O₃-ZrO₂ mixed oxides.

The cumulative pore volume and average pore diameter determined from the desorption isotherm by using the Barrett, Joyner, and Halenda (BJH) method [19] changed with the content of CeO₂ or Y₂O₃ in the mixed oxides. Compared to pure ZrO₂, all the mixed oxides had a smaller cumulative pore volume and average pore diameter. The cumulative pore volumes of CeO₂-ZrO₂ mixed oxides decreased with an increase in CeO₂ content from 12 to 100%. However, the cumulative pore volumes of Y₂O₃-ZrO₂ mixed oxides had little change when the content of Y₂O₃ increased from 2.5 to 12%. All the mixed oxides had a similar average pore diameter ca. 3–5 nm that was in the region of mesoporous pores.

The crystal sizes of the CeO₂- and Y₂O₃-doped ZrO₂ catalysts were all smaller than that of pure ZrO₂, as can be seen from Table 1. It has been reported that the oxides of zirconium form three different phases: monoclinic, tetragonal, and cubic [20–22]. The monoclinic phase is stable below

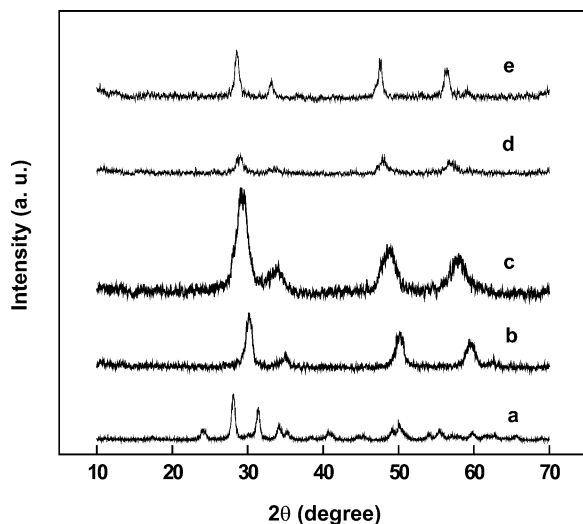


Fig. 1. XRD patterns of $\text{CeO}_2\text{-ZrO}_2$ mixed oxides with (a) 0% CeO_2 , (b) 12% CeO_2 , (c) 50% CeO_2 , (d) 88% CeO_2 , (e) 100% CeO_2 .

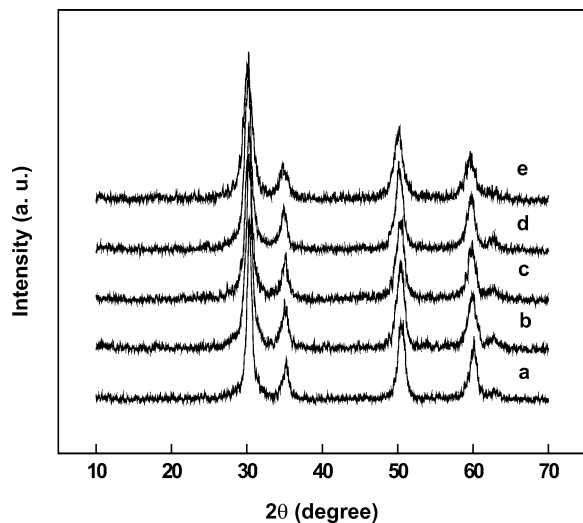


Fig. 2. XRD patterns of $\text{Y}_2\text{O}_3\text{-ZrO}_2$ mixed oxides with (a) 2.5% Y_2O_3 , (b) 4.5% Y_2O_3 , (c) 6.2% Y_2O_3 , (d) 8.6% Y_2O_3 , (e) 12% Y_2O_3 .

1473 K, and the cubic phase is formed at temperatures above 2553 K. The presence of other doping metals in ZrO_2 and the parameters of precipitation play a role in determining the final crystal phase. The crystal phases of the $\text{CeO}_2\text{-ZrO}_2$ and $\text{Y}_2\text{O}_3\text{-ZrO}_2$ mixed oxides were determined by XRD and Raman in this study. The powder X-ray patterns of the catalysts are shown in Figs. 1 and 2. Fig. 1 shows the XRD patterns of $\text{CeO}_2\text{-ZrO}_2$ mixed oxide catalysts. A monoclinic phase (the peaks at $2\theta \sim 28.2^\circ$, 31.5° are assigned to the phase) was the dominating crystal phase for pure ZrO_2 (Fig. 1a) prepared under the conditions used in the study. A small quantity of CeO_2 (12 mol%) added to zirconia remarkably changed the crystal phase. The peaks at $2\theta \sim 28.2^\circ$ and 31.5° (monoclinic) for pure ZrO_2 disappeared while the peak at $2\theta \sim 30^\circ$ increased (Fig. 1b). The diffraction peak at $2\theta \sim 30^\circ$ is assigned to a tetragonal or/and cubic ZrO_2 phase. The charac-

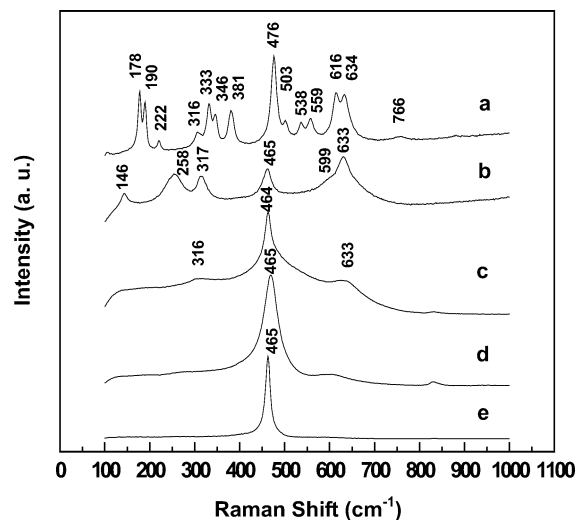


Fig. 3. Raman spectra of $\text{CeO}_2\text{-ZrO}_2$ mixed oxides with (a) 0% CeO_2 , (b) 12% CeO_2 , (c) 50% CeO_2 , (d) 88% CeO_2 , (e) 100% CeO_2 .

teristic peaks for a tetragonal ZrO_2 phase are at $2\theta \sim 30.2$, 34.8 , and 35.2° [23] and those for a cubic ZrO_2 phase are at $2\theta \sim 30$ and 34.8° [24]. The weak and broad diffraction peaks obtained over these catalysts in this study make it difficult to discern a tetragonal phase from a cubic phase. It is evident that CeO_2 and ZrO_2 form a solid solution because a free CeO_2 phase was not observed. The XRD pattern of CeO_2 (Fig. 1e) alone can be assigned to a typical cubic fluorite structure at peaks $2\theta \sim 28.6$ and 33.1° . The diffraction peak at $2\theta \sim 30^\circ$ for 12% CeO_2 -doped ZrO_2 catalyst (Fig. 1b) was shifted to lower 2θ degree with a rise in the quantity of CeO_2 incorporated to ZrO_2 (Figs. 1c and d). This observation indicates an increase of the lattice defects due to the replacement of Zr^{4+} with Ce^{4+} , which coincides with the fact that the cation radius of Ce^{4+} (1.09 Å) is larger than that of Zr^{4+} (0.86 Å).

Fig. 2 shows the XRD patterns of $\text{Y}_2\text{O}_3\text{-ZrO}_2$ mixed oxides. No apparent differences were observed for these catalysts with the content of Y_2O_3 increasing from 2.5 to 12%. The weak and broad diffraction peaks at $2\theta \sim 30$ and 35° can also be assigned to a tetragonal or/and cubic ZrO_2 phase.

Raman spectra of the mixed oxides are shown in Figs. 3 and 4. In contrast to the XRD patterns, which gives information related mainly to the cation sublattice, Raman spectra are dominated by oxygen lattice vibrations [25] and are sensitive to the crystalline symmetry, thus being a useful tool for obtaining additional structural information of multioxide systems exhibiting lattice disorder. Fig. 3 shows the Raman spectra of $\text{CeO}_2\text{-ZrO}_2$ mixed oxides. The spectrum of pure ZrO_2 (Fig. 3a) featured several bands in the region which are attributable to monoclinic ZrO_2 [26], while one sharp single band (located at 465 cm^{-1}) characterizes the Raman spectrum of pure CeO_2 (Fig. 3e). This peak at 465 cm^{-1} is due to the F_{2g} Raman-active mode typical of a cubic fluorite-structured material [27]. Six bands at approx-

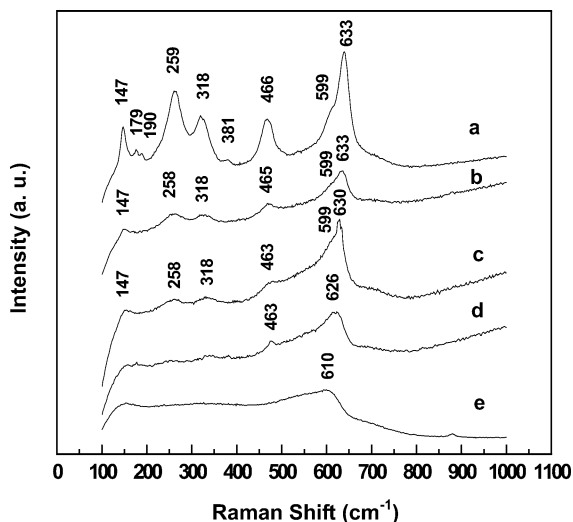


Fig. 4. Raman spectra of $\text{Y}_2\text{O}_3\text{-ZrO}_2$ mixed oxides with (a) 2.5% Y_2O_3 , (b) 4.5% Y_2O_3 , (c) 6.2% Y_2O_3 , (d) 8.6% Y_2O_3 , (e) 12% Y_2O_3 .

imately 633 , 599 , 465 , 317 , 258 , and 146 cm^{-1} observed for 12% CeO_2 -doped ZrO_2 catalyst (Fig. 3b) are predicated for a typical tetragonal ZrO_2 [28]. The Raman spectrum of 50% CeO_2 -doped ZrO_2 catalyst (Fig. 3c) was assigned to a pseudo-cubic tetragonal (t'') phase and it is characterized by an intense peak at 465 cm^{-1} and weak bands at 316 and 633 cm^{-1} [25]. A 88% CeO_2 -doped ZrO_2 catalyst featured one sharp peak at 465 cm^{-1} and it was assigned to a cubic CeO_2 phase. The broadness of the peak in the case of Fig. 3d, compared to pure CeO_2 (Fig. 3e) is probably caused by the small crystallites generated by the incorporation of ZrO_2 into CeO_2 crystal lattice [29].

The Raman spectra of $\text{Y}_2\text{O}_3\text{-ZrO}_2$ mixed oxides are presented in Fig. 4. With the content of Y_2O_3 in the mixed oxides lower than 8.6 mol%, the samples all showed Raman spectra characteristic of tetragonal zirconia with six typical peaks (Figs. 4a, b, and c). The further three bands, located at 381 , 190 , and 179 cm^{-1} , indicate that a small quantity of monoclinic ZrO_2 is still present for 2.5% Y_2O_3 -doped ZrO_2 mixed oxide (Fig. 4a). As shown in Fig. 4, the characteristic bands of tetragonal phase markedly faded with an increase in the content of Y_2O_3 . It indicates a decrease of a tetragonal phase in the mixed oxides with an increase in Y_2O_3 content. The peak at 633 cm^{-1} which is ascribed to the vibrations in the monoclinic, tetragonal, and cubic ZrO_2 phase [30] did not change significantly but shifted to lower wavenumbers when the content of Y_2O_3 increased from 4.5 to 8.6% (Figs. 4b, c, and d). It would suggest that a cubic phase coexisted with a tetragonal phase in these mixed oxides. When the content of Y_2O_3 was increased to 12%, the bands characterized for a tetragonal phase disappeared with one broad peak at ca. 610 cm^{-1} which was assigned to a cubic ZrO_2 phase [30]. The Raman spectrum of pure Y_2O_3 features a strong band at around 375 cm^{-1} [31]. The absence of the peak at 375 cm^{-1} in Fig. 4 indicates that all

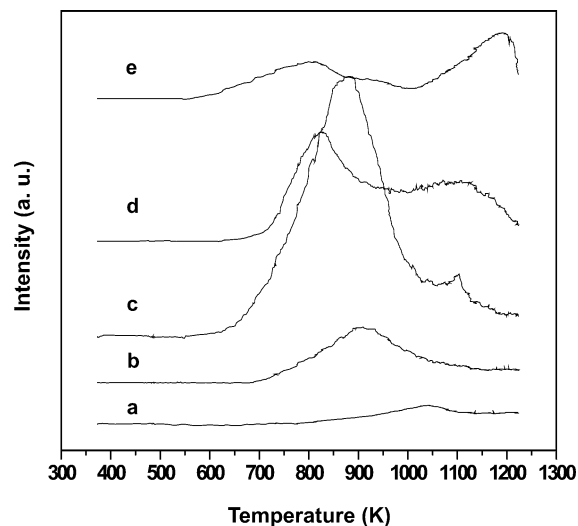


Fig. 5. H_2 -TPR profiles of $\text{CeO}_2\text{-ZrO}_2$ mixed oxides with (a) 0% CeO_2 , (b) 12% CeO_2 , (c) 50% CeO_2 , (d) 88% CeO_2 , (e) 100% CeO_2 .

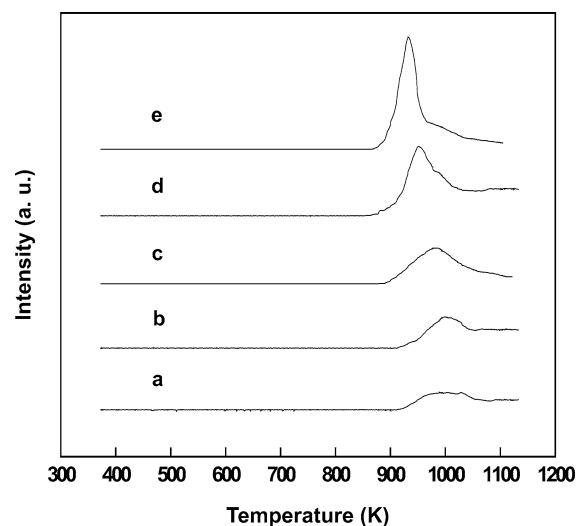


Fig. 6. H_2 -TPR profiles of $\text{Y}_2\text{O}_3\text{-ZrO}_2$ mixed oxides with (a) 2.5% Y_2O_3 , (b) 4.5% Y_2O_3 , (c) 6.2% Y_2O_3 , (d) 8.6% Y_2O_3 , (e) 12% Y_2O_3 .

the Y_2O_3 -doped ZrO_2 oxides formed solid solutions in this investigation.

3.2. Chemical properties of the mixed oxide catalysts

The reduction behavior of $\text{CeO}_2\text{-ZrO}_2$ and $\text{Y}_2\text{O}_3\text{-ZrO}_2$ mixed oxides were investigated by means of the H_2 -TPR technique and the TPR profiles are presented in Figs. 5 and 6. The quantities of H_2 consumption per gram catalyst were calculated and presented in Figs. 7 and 8 as a function of content of CeO_2 and Y_2O_3 in the mixed oxides, repetitively. Fig. 5 shows the TPR results of the $\text{CeO}_2\text{-ZrO}_2$ mixed oxides. It can be seen that only a small quantity of H_2 was consumed on pure ZrO_2 (Fig. 5a), as reported in other literature [32]. The incorporation of CeO_2 to ZrO_2 greatly enhanced the reduction behavior of ZrO_2 . The quantities of H_2 consumption increased with an increase in the content

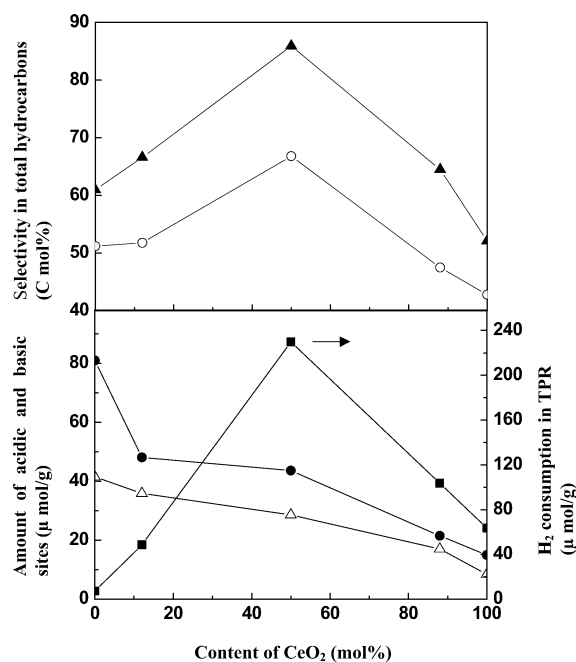


Fig. 7. Quantities of H₂ consumption, amount of acidic and basic sites, and selectivities of C₄ and i-C₄ in total hydrocarbons as a function of content of CeO₂ in CeO₂–ZrO₂ mixed oxide catalysts. ■, Quantity of H₂ consumption in TPR; △, amount of acidic sites; ●, amount of basic sites; ▲, C₄ selectivity in total hydrocarbons; ○, i-C₄ selectivity in total hydrocarbons.

of CeO₂ up to a maximum at about 50% (Fig. 5c), and then decreased with more CeO₂ added. This enhancement of H₂ consumption could be attributed to an increase of the lattice oxygen mobility in the bulk of CeO₂–ZrO₂ solid solution because of the distortion of the ZrO₂ structure by the incorporation of CeO₂ and then the lattice oxygen would be more active to react with H₂, although surface and bulk reduction of CeO₂–ZrO₂ mixed oxides cannot be distinguished by the conventional TPR technique [13,32–34]. A single peak was observed for a 12% CeO₂-doped ZrO₂ catalyst (Fig. 5b). For pure CeO₂ (Fig. 5e), two TPR peaks were observed at ca. 800 and 1160 K. These two peaks were also reported in other studies and were interpreted to correspond with the reduction of the easily reducible surface oxygen and the bulk oxygen, respectively [35]. Although similar to that of pure CeO₂, two peaks were observed over both 50% CeO₂ (Fig. 5c) and 88% CeO₂ (Fig. 5d)-doped ZrO₂ catalysts and the main peaks for H₂ consumption were shifted to a lower temperature region compared with that over pure CeO₂. Furthermore, the main peaks for H₂ consumption over 12% CeO₂-, 50% CeO₂-, and 88% CeO₂-doped ZrO₂ mixed oxides remarkably shifted to lower temperatures compared to that over pure ZrO₂. This implies that the mobility of lattice oxygen was enhanced and then could be more easily reduced because of the distortion of the oxygen sublattice in these CeO₂–ZrO₂ mixed oxides.

The TPR patterns of Y₂O₃–ZrO₂ mixed oxides are shown in Fig. 6. It can be seen that the intensity of the reduction peak increased with an increase of Y₂O₃ content up to 8.6%.

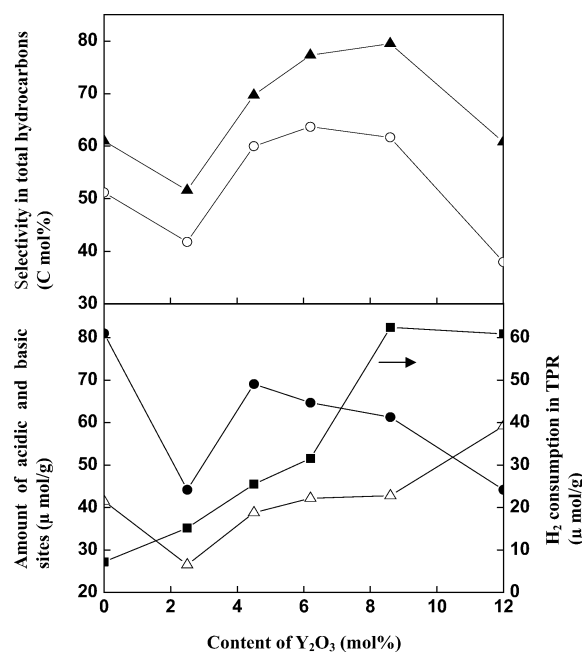


Fig. 8. Quantities of H₂ consumption, amount of acidic and basic sites, and selectivities of C₄ and i-C₄ in total hydrocarbons as a function of content of Y₂O₃ in Y₂O₃–ZrO₂ mixed oxide catalysts. ■, Quantity of H₂ consumption in TPR; △, amount of acidic sites; ●, amount of basic sites; ▲, C₄ selectivity in total hydrocarbons; ○, i-C₄ selectivity in total hydrocarbons.

No significant increase in the quantity of H₂ consumption was obtained over a 12% Y₂O₃-doped ZrO₂ catalyst compared to that over a 8.6% Y₂O₃-doped ZrO₂ catalyst, as shown in Fig. 8. This is coincident with the results reported in the literature [36] that the maximum electrical conductivity, with diffusing oxygen ions being the primary charge carrier, was obtained at a Y₂O₃ content of ca. 9–10%. Similar to the TPR patterns of CeO₂–ZrO₂ mixed oxides, the TPR peaks of these Y₂O₃–ZrO₂ mixed oxides also shifted to lower temperatures with an increase in the amount of Y₂O₃ doped. Pure Y₂O₃ cannot be reduced by H₂ until 1123 K in the TPR [37].

From the TPR results presented in Figs. 5 and 6, it can be concluded that the reduction behavior of the CeO₂–ZrO₂ and Y₂O₃–ZrO₂ catalysts was largely improved compared to that of pure ZrO₂ catalyst. The enhanced reduction behavior is suggested to be related to the increased mobility of lattice oxygen of the catalysts [13–16,32]. It has been reported that a condensation reaction [38], which takes place between an η³-enolate and a methoxy species on the ZrO₂ catalysts [7], primarily contributes to C₄ and C₄₊ products, which explains the reason for the deviation of the isosynthesis product distribution from the typical Schulz–Flory–Anderson distribution observed for Fischer–Tropsch synthesis. The enhancement of the mobility of lattice oxygen of these CeO₂- or Y₂O₃-doped ZrO₂ catalysts would be likely to play an important role in the isosynthesis if the formation of the intermediate substances for the condensation reaction, η³-enolate and methoxy species, is influenced by the lattice oxygen because these two substances both have oxy-

Table 2
Catalytic performance of CeO₂–ZrO₂ mixed oxide catalysts in the isosynthesis^a

Content of CeO ₂ ^b (mol%)	CO conversion (%)	Selectivity (C mol%)			Distribution of hydrocarbons (C mol%)					i-C ₄ /CH ^c (C mol%)
		CH ^c	CHO ^d	CO ₂	C ₁	C ₂	C ₃	C ₄	C ₅₊	
0	16.5	50.8	10.1	39.1	3.1	8.9	3.8	61.0	23.2	51.2
12	18.2	47.6	6.8	45.6	8.6	7.9	6.0	66.6	10.9	51.8
50	22.8	51.3	2.0	46.7	5.4	2.6	3.0	85.9	3.0	66.8
88	16.6	54.9	0	45.1	12.6	7.0	5.5	64.5	10.4	47.5
100	12.1	54.5	0	45.5	23.5	11.3	6.2	52.1	6.9	42.8

^a Reaction conditions: 673 K, 5.0 MPa, GHSV = 650 h⁻¹, CO/H₂ = 1.

^b CeO₂/(CeO₂ + ZrO₂).

^c Hydrocarbons.

^d CH₃OH + CH₃OCH₃.

^e i-C₄ selectivity in total hydrocarbons.

Table 3
Catalytic performance of Y₂O₃–ZrO₂ mixed oxide catalysts in the isosynthesis^a

Content of Y ₂ O ₃ ^b (mol%)	CO conversion (%)	Selectivity (C mol%)			Distribution of hydrocarbons (C mol%)					i-C ₄ /CH ^c (C mol%)
		CH ^c	CHO ^d	O ₂	C ₁	C ₂	C ₃	C ₄	C ₅₊	
2.5	13.9	50.8	7.3	41.9	16.7	9.1	5.5	51.6	17.1	41.8
4.5	17.0	49.2	8.5	42.3	5.4	8.6	2.0	69.7	14.2	60.0
6.2	18.8	51.9	5.0	43.1	4.9	7.5	1.5	77.3	8.7	63.7
8.6	23.2	55.1	5.1	39.8	3.4	7.4	1.5	79.5	8.0	61.7
12.0	22.6	47.6	8.8	43.6	12.1	11.1	7.8	60.8	8.2	38.0

^a Reaction conditions: 673 K, 5.0 MPa, GHSV = 650 h⁻¹, CO/H₂ = 1.

^b Y₂O₃/(Y₂O₃ + ZrO₂).

^c Hydrocarbons.

^d CH₃OH + CH₃OCH₃.

^e i-C₄ selectivity in total hydrocarbons.

gen atoms which may come from the lattice oxygen of the catalysts [39].

The acid and base characteristics of the catalysts were measured by NH₃-TPD and CO₂-TPD, respectively. ZrO₂ has been well known as a bifunctional catalyst with both weak acid and base sites [40]. In present work, the weakly acidic and weakly basic properties of the surface of zirconia were indicated by these desorption peaks of NH₃-TPD and CO₂-TPD at temperatures lower than 573 K, respectively. No significant differences were observed on the desorption temperatures of NH₃ and CO₂ between the CeO₂–ZrO₂ or Y₂O₃–ZrO₂ mixed oxides and pure ZrO₂. However, the amount of acidic and basic sites markedly varied with the types and the quantities of dopants added, as shown in Figs. 7 and 8. It can be seen that the amount of acidic and basic sites for CeO₂–ZrO₂ mixed oxides both remarkably decreased with an increase in the content of CeO₂ (Fig. 7). The TPD results of pure CeO₂ (content of CeO₂ at 100%, Fig. 7) showed that CeO₂ possessed a much lesser amount of acidic and basic sites which are only one-fifth of that over pure ZrO₂ (content of CeO₂ at 0%, Fig. 7) in this study. For Y₂O₃–ZrO₂ mixed oxides, the changing trend in the amount of acid–base sites with the content of Y₂O₃ was a little different from that of CeO₂–ZrO₂ catalysts. It was found that the amount of acidic and basic sites both largely decreased when 2.5% Y₂O₃ was doped with ZrO₂ compared with that over pure ZrO₂ (Fig. 8). Then, the amount of acidic sites in-

creased slightly with more and more Y₂O₃ doped. However, the amount of basic sites decreased with an increase in the content of Y₂O₃ from 4.5 to 12%. It is not clear what caused a 2.5% Y₂O₃-doped ZrO₂ catalyst to have so small quantities of basic sites.

3.3. Catalytic performance of the mixed oxide catalysts

The results of the catalytic test of the CeO₂–ZrO₂ and Y₂O₃–ZrO₂ mixed oxide catalysts in the CO hydrogenation at 673 K, 5.0 MPa, and 650 h⁻¹ are presented in Tables 2 and 3. Under the reaction conditions in this study, the predominant catalytic reaction products consisted of hydrocarbons, CO₂, methanol, and dimethyl ether (DME). Table 2 shows the catalytic performance of CeO₂–ZrO₂ mixed oxide catalysts. About 16.5% CO was converted with 51% i-C₄ selectivity in total hydrocarbons over pure ZrO₂ catalysts. The lower selectivity to C₁–C₃ hydrocarbons than that reported in the literature under the similar reaction conditions [6–10] is ascribed to the quartz-lined stainless-steel tubular reactor used in this study. Our previous work [18] has indicated that the catalytic performance of the catalysts was seriously affected with an additional production of mainly C₁–C₃ hydrocarbons in the stainless-steel tubular reactor. As can be seen from Table 2, the activities and selectivities of the catalysts markedly varied with the content of CeO₂ doped. It is interested to note that the activity and C₄ and i-C₄ selectiv-

ity in total hydrocarbons all reached a maximum over 50% CeO₂-doped ZrO₂ catalyst. Pure CeO₂ was also active for the isosynthesis with *i*-C₄ selectivity in total hydrocarbons ca. 42%. However, the selectivity to CH₄ in total hydrocarbons was much higher than that over pure ZrO₂ catalyst with a low selectivity to C₅₊ hydrocarbons over pure CeO₂. The CO₂ selectivities in the products over CeO₂-doped ZrO₂ catalysts were all higher than that over pure ZrO₂ with a low selectivities to CH₃OH + DME (CHO).

The tested results of Y₂O₃-ZrO₂ mixed oxide catalysts in the isosynthesis are shown in Table 3. It can be seen that the activities of the catalysts increased with an increase in the content of Y₂O₃ doped. However, no significant difference in activities was observed when the content of Y₂O₃ was increased from 8.6 to 12%. The C₄ selectivity in total hydrocarbons reached a maximum at a content of Y₂O₃ ca. 8.6%, while the maximum *i*-C₄ selectivity in total hydrocarbons was obtained over the 6.2% Y₂O₃-doped ZrO₂ catalyst. As CeO₂-doped ZrO₂ catalysts shown in Table 2, higher CO₂ selectivities with lower CHO selectivities were also obtained over all the Y₂O₃-doped ZrO₂ catalysts compared to that over pure ZrO₂. But the CO₂ selectivities were a little lower than that over CeO₂-doped ZrO₂ catalysts shown in Table 2.

3.4. Relationship between catalytic performance and physical-chemical properties of the ZrO₂-based catalysts

It is known that a high catalytic activity can be more likely obtained on a catalyst with a high surface area if the catalysts exhibit a similar chemical structure and acid–base behavior because of the larger contact surface with reactants over the catalyst with a higher surface area. However, the higher CO conversion obtained over the 50% CeO₂ and 8.6% Y₂O₃-doped ZrO₂ catalysts cannot be explained alone by the enhancement of surface areas for these two catalysts because some other catalysts with similar high surface areas, such as 4.5% Y₂O₃-doped ZrO₂ catalyst, performed much lower activities to CO hydrogenation. In the same way, a relationship between the cumulative pore volumes or average pore diameters and the catalytic performances of the catalysts was not found in this investigation.

It has been reported that the crystal phase had an effect on the isosynthesis that isobutene formed on the monoclinic phase over ZrO₂ [12]. However, tetragonal and cubic phases were the main crystal phase for the catalysts prepared in this study except for pure ZrO₂ on which a monoclinic phase was the predominant phase. So the improvement of the catalytic performance on some CeO₂- and Y₂O₃-doped ZrO₂ catalysts cannot be interpreted from the crystal phases of the catalysts. No significant differences in the crystal sizes of the doped catalysts were observed, as shown in Table 1. It may be speculated that there would be other more important factors that govern the performance of the catalysts in the isosynthesis.

The dependencies of isosynthesis activities and selectivities on acid–base properties of ZrO₂-based catalysts have

been widely investigated [5–10]. The acidic and basic sites have been suggested to be the active sites for the isosynthesis. The promoting effects of various calcium salts or Al₂O₃-KOH doped into ZrO₂ on the isosynthesis reaction were studied in our previous works [9,10]. The physical properties, such as surface areas, particle sizes, and crystal phases, were very similar for those promoted ZrO₂-based catalysts due to the mechanical mixing method used to prepare those doped catalysts. The TPR patterns of the calcium salts or Al₂O₃-KOH-promoted ZrO₂-based catalysts (not presented) showed similar H₂ consumptions as those of pure ZrO₂ catalysts. A little increase of H₂ consumption over Al₂O₃-KOH-promoted ZrO₂-based catalysts is attributed to the reduction of KOH ca. 0.5% doped. However, the amount of acid and base sites on those catalysts remarkably varied. Therefore, the effects of acid–base properties on the performance of catalysts could be identified. The basic sites were found to be significant for the formation of *i*-C₄ hydrocarbons [9,10]. The importance of basic sites in the isosynthesis has also been reported by other researchers [5,6]. However, the CO₂-TPD results in this study (Figs. 7 and 8) showed that the amounts of the basic sites on the CeO₂-ZrO₂ and Y₂O₃-ZrO₂ catalysts were all lower than that on the pure ZrO₂ catalysts. The tested results of isosynthesis reported in Tables 2 and 3 show that the selectivities to *i*-C₄ hydrocarbons over some catalysts, such as 50% CeO₂ and 6.2% Y₂O₃-doped ZrO₂ catalysts were remarkably higher than that over pure ZrO₂ catalysts. Therefore, this improvement of *i*-C₄ selectivities in total hydrocarbons could not be solely explained by the acid–base properties on the catalysts in this study.

The selectivities to C₄ and *i*-C₄ in total hydrocarbons are also presented in Figs. 7 and 8 as a function of the content of CeO₂ or Y₂O₃ doped in the catalysts. It is interesting to note that the highest selectivities to C₄ in total hydrocarbons were obtained over the catalysts which have a maximum quantity of H₂ consumption in the TPR for both CeO₂-ZrO₂ and Y₂O₃-ZrO₂ mixed oxide catalysts. The maximum levels were at 50% CeO₂ and 8.6% Y₂O₃ doped, respectively. The selectivity to *i*-C₄ in total hydrocarbons also achieved a maximum over 50% CeO₂-doped ZrO₂ catalyst for the CeO₂-ZrO₂ mixed oxide catalysts (Fig. 7). However, high selectivities to *i*-C₄ in total hydrocarbons were obtained over the catalysts with the contents of Y₂O₃ doped ranging from 4.5 to 8.6% for the Y₂O₃-ZrO₂ mixed oxide catalysts, as shown in Fig. 8. No direct relationship between the amount of acidic or basic sites and the selectivities to C₄ and *i*-C₄ in total hydrocarbons was observed for the CeO₂- or Y₂O₃-doped ZrO₂ catalysts, as shown in Figs. 7 and 8. Therefore, the improvement of catalytic performance over some CeO₂- or Y₂O₃-doped ZrO₂ catalysts could be attributed to the enhancement of redox properties that are suggested to be related to the increased mobility of lattice oxygen of the catalysts [13–16,32].

It has been proposed that there are two independent paths, CO insertion and condensation reaction, for the chain prop-

agation reactions leading to C_{2+} hydrocarbons over ZrO_2 -based catalysts [38,41]. The CO insertion step comprises the addition of a CO molecule into the Zr–C bond of a surface aldehydic intermediate. Hence, the product distribution should be that which could be predicted from a typical Schulz–Flory–Anderson (S–F–A) distribution [1]. The condensation reaction comprises the condensation of a surface-bound enolate with a surface alkoxy species [42]. A condensation reaction which primarily contributes to C_4 and C_{4+} products [7] is suggested to be responsible for the deviations from the S–F–A product distribution for the isosynthesis reaction. In this study, the observed remarkable enhancement of C_4 selectivity in total hydrocarbons is due to the improvement of condensation reaction by an enhancement in mobility of lattice oxygen in these catalysts, although it is not clear how the active lattice oxygen influences the condensation reaction.

However, the quantity of active lattice oxygen cannot be assigned to be the only factor in determining the performance of the catalysts. As can be seen in Fig. 8, the highest $i-C_4$ selectivity in total hydrocarbons was achieved over 6.2% Y_2O_3 -doped ZrO_2 -based catalysts, not 8.6% Y_2O_3 -nor 12% Y_2O_3 -doped catalysts which both have the maximum quantity of active lattice oxygen for the Y_2O_3 - ZrO_2 mixed oxide catalysts. It was also found that the selectivities to C_4 and $i-C_4$ in total hydrocarbons showed a sharp decline with more C_1 and C_2 hydrocarbons (Table 3) when the content of Y_2O_3 was increased from 8.6 to 12%, although an almost same quantity of H_2 consumption in the TPR was obtained over these two catalysts. This would be ascribed to the large decrease of basic sites on the 12% Y_2O_3 -doped ZrO_2 catalyst as can be seen in Fig. 8 since basic sites have been extensively reported to be significant for the formation of $i-C_4$ hydrocarbons [6,9,12]. The marked decrease of basic sites can also explain the decrease of $i-C_4$ selectivities in total hydrocarbons for the 88% CeO_2 - and 2.5% Y_2O_3 -doped ZrO_2 catalysts, as shown in Figs. 7 and 8, respectively.

We have identified the effects of acid–base properties on the activity and selectivity of the ZrO_2 -based catalysts which have similar physical and redox properties but different acid–base properties [9]. Higher isosynthesis activities were obtained over the catalysts with more acidic sites. In this investigation, the differences in activities for the catalysts cannot be ascribed to the amount of acidic sites alone. Some catalysts, such as 50% CeO_2 - and 8.6% Y_2O_3 -doped ZrO_2 catalysts, which have a lesser or similar amount of acidic sites compared to pure ZrO_2 , had much higher isosynthesis activities than those over pure ZrO_2 catalyst. The increase in activity is due to the enhancement of active lattice oxygen of the catalysts because it has been indicated that increasing active lattice oxygen improved one of the chain propagation reactions, condensation, to produce more C_4 hydrocarbons.

The relationships between the ratio of base/acid sites on CeO_2 - ZrO_2 and Y_2O_3 - ZrO_2 catalysts and the $i-C_4/n-C_4$ ratio for the CeO_2 - or Y_2O_3 -doped ZrO_2 catalysts are pre-

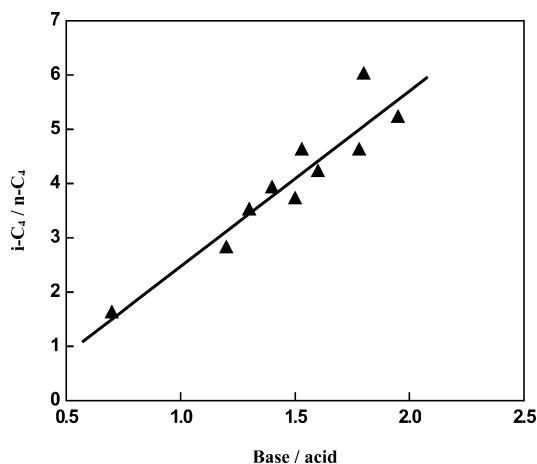


Fig. 9. Ratio of $i-C_4/n-C_4$ as a function of base site/acid site ratio for CeO_2 - ZrO_2 and Y_2O_3 - ZrO_2 mixed oxide catalysts.

sented in Fig. 9. The changing trends that the ratio of $i-C_4/n-C_4$ increased with increasing ratio of base/acid sites are consistent with the results reported in our previous works [9,10]. The ratios of $i-C_4/n-C_4$ were also plotted as a function of the quantities of H_2 consumption over CeO_2 - or Y_2O_3 -doped ZrO_2 catalysts, but no apparent relationships were found. It suggests that the formation of $n-C_4$ and $i-C_4$ requires different active, acidic, and basic sites, respectively. The ratio of base/acid sites would determine the percentages of $i-C_4$ and $n-C_4$ in total C_4 hydrocarbons [9,10].

The importance of a coordination of active lattice oxygen and acid–base of the catalysts for the isosynthesis reaction is emphasized in this paper. The role of active lattice oxygen is to increase the quantities of the condensation reaction intermediates, such as methoxy or η^3 -enolates, or to stabilize these intermediates leading to the production of C_4 hydrocarbons. Acidic sites and basic sites are also required for the formation of C_4 hydrocarbons. A large decrease in the amount of acid and base sites would lead to a decline of C_4 productions, as indicated by the 2.5% Y_2O_3 -doped ZrO_2 -based catalyst, although it has a higher quantity of active lattice oxygen than pure ZrO_2 catalyst. The importance of acidic and basic properties for the formation of C_4 hydrocarbons has been also indicated in the literature. Jackson et al. [43] found that the greater percentage of C_4 products was obtained over the catalysts with more acidity. However, Maruya et al. [5] found that increasing basicity promoted the formation of C_4 hydrocarbons, especially isobutene. In this study, the acidic sites and basic sites are suggested to be the active sites for the formation of $n-C_4$ and $i-C_4$ hydrocarbons, respectively. The ratio of base to acid sites would determine the percentages of $i-C_4$ and $n-C_4$ in total C_4 hydrocarbons, as indicated in Fig. 9. Lower ratios of base to acid sites leads to a higher $n-C_4$ percentage in total C_4 hydrocarbons, as indicated by 12% Y_2O_3 -doped ZrO_2 catalyst (Table 3). The results in this study do not contradict those reported by Jackson et al. [43] and Maruya et al. [5]. In fact, $n-C_4$ hydrocarbons were the main C_4 products (branched/linear ratio lower

than 1) in the work of Jackson [43] using the catalysts with more acidity. *i*-C₄ hydrocarbons were the main products in the C₄ hydrocarbons for the basic oxide-promoted ZrO₂ catalysts prepared by Maruya et al. [5]. The improvement of C₄ and *i*-C₄ selectivities in total hydrocarbons over some CeO₂- or Y₂O₃-doped catalysts is attributed to the enhancement of the quantity of active lattice oxygen of the catalysts meanwhile maintaining an appropriate amount of acid and base sites and ratio of base to acid sites on these catalysts.

4. Conclusions

The incorporation of CeO₂ or Y₂O₃ with ZrO₂ by coprecipitation changed the redox and acid–base properties of ZrO₂-based catalysts and subsequently affected the catalytic performance in the isosynthesis reaction. The enhanced redox properties of zirconia-based catalysts may be ascribed to an increased lattice oxygen mobility of the catalysts for a distortion of the oxygen sublattice by the incorporation of Ce⁴⁺ or Y³⁺ into the zirconia lattice. Active lattice oxygen and acid–base properties are identified to be responsible for the condensation reaction leading to the production of C₄ hydrocarbons. The ratio of base to acid sites determines the percentage of *n*-C₄ and *i*-C₄ in total C₄ hydrocarbons for the isosynthesis reaction. A coordination of quantity of active lattice oxygen and acid–base properties accounts for the remarkable improvement of isosynthesis activities and selectivities over some CeO₂- or Y₂O₃-doped ZrO₂-based catalysts.

Acknowledgments

Financial support of this study is provided by the National Natural Science Foundation of China and the Analytical Foundation of Tsinghua University.

References

- [1] A. Sofianos, *Catal. Today* 15 (1992) 149.
- [2] H. Pichler, K.H. Ziesecke, *Brennst. Chem.* 30 (1949) 13.
- [3] H. Pichler, K.H. Ziesecke, *Brennst. Chem.* 30 (1949) 60.
- [4] T. Maehashi, K. Maruya, K. Domen, K. Aika, T. Onishi, *Chem. Lett.* (1984) 747.
- [5] K. Maruya, T. Maehashi, T. Haraoka, S. Narui, Y. Asakawa, K. Domen, T. Onishi, *Bull. Chem. Soc. Jpn.* 61 (1988) 667.
- [6] Z.T. Feng, W.S. Postula, A. Akgerman, R.G. Anthony, *Ind. Eng. Chem. Res.* 34 (1995) 78.
- [7] N.B. Jackson, J.G. Ekerdt, *J. Catal.* 126 (1990) 31.
- [8] C.L. Su, J.R. Li, D.H. He, Z.X. Cheng, Q.M. Zhu, *Appl. Catal.* 202 (2000) 81.
- [9] Y.W. Li, D.H. He, Z.X. Cheng, C.L. Su, J.R. Li, Q.M. Zhu, *J. Mol. Catal.* 175 (2001) 267.
- [10] Y.W. Li, D.H. He, Y.B. Yuan, Z.X. Cheng, Q.M. Zhu, *Energy Fuels* 15 (2001) 1434.
- [11] K. Tanabe, *Mater. Chem. Phys.* 13 (1985) 347.
- [12] K. Maruya, T. Komiya, K. Okumura, M. Yashima, *Chem. Lett.* (1999) 575.
- [13] G. Vlaic, P. Fornasiero, S. Geremia, J. Kaspar, M. Graziani, *J. Catal.* 168 (1997) 386.
- [14] G. Vlaic, D. Monte, P. Fornasiero, E. Fonda, J. Kaspar, M. Graziani, *J. Catal.* 182 (1999) 378.
- [15] T.H. Etsell, S.N. Flengas, *Chem. Rev.* 70 (1970) 339.
- [16] R.G. Silver, C.J. Hou, J.G. Ekerdt, *J. Catal.* 118 (1989) 400.
- [17] B.D. Cullity, in: M. Cohen (Ed.), *Elements of X-Ray Diffraction*, 2nd ed., Addison–Wesley, Reading, MA, 1978, p. 285.
- [18] Y.W. Li, D.H. He, Q.M. Zhu, *Abstracts of Papers of the American Chemical Society* 223, 087-FUEL Part 1, 2002.
- [19] E.P. Barret, L.G. Joyner, P.P. Halenda, *J. Am. Chem. Soc.* 73 (1951) 373.
- [20] J.D. McCullough, K.N. Trueblood, *Acta Crystallogr.* 12 (1959) 507.
- [21] P.A. Evans, R. Stevens, J.G.P. Binner, *Trans. J. Br. Ceram. Soc.* 83 (1984) 39.
- [22] H.G. Scott, *J. Mater. Sci.* 10 (1975) 1527.
- [23] U. Martin, H. Boysen, F. Frey, *Acta Crystallogr., Sect. B: Struct. Sci.* 49 (1993) 403.
- [24] A. Chatterjee, S.K. Pradhan, A. Datta, M. De, D.J. Chakravorty, *Mater. Res.* 9 (1994) 263.
- [25] J.R. Ferraro, K. Nakamoto, *Introductory Raman Spectroscopy*, Academic Press, New York, 1994.
- [26] V.G. Keramidis, W.B. White, *J. Am. Ceram. Soc.* 57 (1974) 22.
- [27] A. Trovarelli, F. Zamar, J. Lorca, C. Leitenburg, G. Dolcetti, J.T. Kiss, *J. Catal.* 169 (1997) 490.
- [28] D.J. Kim, H.J. Jung, I.N. Yang, *J. Am. Ceram. Soc.* 76 (1993) 2106.
- [29] H. Richter, Z.P. Wang, L. Levy, *Solid State Commun.* 39 (1981) 625.
- [30] A. Feinberg, C.H. Perry, *J. Phys. Chem. Solids* 42 (1981) 513.
- [31] J.M. Calderon-Moreno, M. Yoshimura, *Solid State Ionics* 154–155 (2002) 125.
- [32] K. Otsuka, Y. Wang, M. Nakamura, *Appl. Catal. A* 183 (1999) 317.
- [33] P. Fornasiero, G. Balducci, R. Monte, J. Kašpar, V. Sergo, G. Gubitosa, A. Ferrero, M. Graziani, *J. Catal.* 164 (1996) 173.
- [34] M. Daturi, E. Finocchio, C. Binet, J.C. Lavalley, F. Fally, V. Perrichon, H. Vidal, N. Hickey, J. Kašpar, *J. Phys. Chem. B* 104 (2000) 9186.
- [35] A. Trovarelli, *Catal. Rev. Sci. Eng.* 38 (1996) 439.
- [36] T.H. Etsell, S.N. Flengas, *Chem. Rev.* 70 (1970) 339.
- [37] W.P. Dow, Y.P. Wang, T.J. Huang, *J. Catal.* 160 (1996) 155.
- [38] T.J. Mazanec, *J. Catal.* 98 (1986) 115.
- [39] N.B. Jackson, J.G. Ekerdt, *J. Catal.* 101 (1986) 90.
- [40] B.Q. Xu, T. Yamaguchi, K. Tanabe, *Chem. Lett.* (1988) 1663.
- [41] S.C. Tseng, N.B. Jackson, J.G. Ekerdt, *J. Catal.* 109 (1988) 284.
- [42] J.G. Nunan, C.E. Bogdan, K. Klier, K.J. Smith, C.W. Young, R.G. Herman, *J. Catal.* 116 (1989) 195.
- [43] N.B. Jackson, J.G. Ekerdt, *J. Catal.* 126 (1990) 46.